Journal of Archaeological Science: Reports 53 (2024) 104403

Contents lists available at ScienceDirect

Journal of Archaeological Science: Reports

journal homepage: www.elsevier.com/locate/jasrep

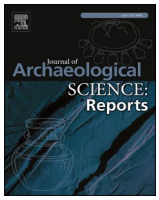

Trace element concentrations as proxies for diagenetic alteration in the African archaeofaunal record: Implications for isotope analysis

Alex Bertacchi [a,*], Andrew M. Zipkin [b,c], Julia Giblin [d], Gwyneth Gordon [e,f], Tyler Goepfert [f], Dan Asael [g], Kelly J. Knudson [b]

[a] Department of Anthropology, Yale University, New Haven, CT, USA
[b] School of Human Evolution and Social Change, Arizona State University, Tempe, AZ, USA
[c] Eurofins, EAG Laboratories, Liverpool, NY, USA
[d] Department of Sociology, Criminal Justice, and Anthropology, Quinnipiac University, Hamden, CT, USA
[e] School of Earth and Space Exploration, Arizona State University, AZ, USA
[f] Knowledge Enterprise, Arizona State University, Tempe, AZ, USA
[g] Department of Earth and Planetary Sciences, Yale University, New Haven, CT, USA

ARTICLE INFO

Keywords:
Enamel
Ostrich eggshell
Maximum threshold concentrations
Isotope ratio
Rb/Sr
LA-MC-ICP-MS
Archaeometry

ABSTRACT

Isotope ratio analyses of trace elements are applied to tooth enamel, ostrich eggshell, and other archaeological hard tissues to infer mobility and other aspects of hominin and animal paleoecology. It has been assumed that these highly mineralized tissues are resistant to diagenetic alteration, but this is seldom tested and some studies document diagenetic alteration over brief time spans. Here, we build on existing research on Maximum Threshold Concentrations (MTCs) to develop screening tools for diagenesis that can inform heavy isotopic analyses. The premise of the MTC approach is that archaeological tissues are likely contaminated and unsuitable for isotope ratio analysis when they exceed characteristic modern concentration ranges of trace elements. Furthermore, we propose a new metric called the Maximum Threshold Ratio (MTR) of $^{85}Rb/^{88}Sr$ or whole element Rb/Sr, which can be measured simultaneously with $^{87}Sr/^{86}Sr$ during laser ablation (LA) MC-ICP-MS or applied during *post hoc* screening of specimens. We analyzed 56 enamel samples from modern Kenyan mammals and 34 modern ostrich eggshells from South Africa, Namibia, and the United States by solution ICP-MS, as well as a subset of shells using LA-MC-ICP-MS. Our results indicate that thresholds are consistent across taxa at a single location, but likely vary across locations. Therefore, MTCs and MTRs need to be tissue and locality specific, but not necessarily taxon-specific. Other important differences are observed between the inner and outer surfaces of the eggshells and between LA and solution ICP-MS. This exploratory study provides guidelines for building reference thresholds to screen enamel and eggshell for diagenesis potentially impacting biogenic isotope ratios.

1. Introduction

Isotopic analysis of trace elements (e.g., Sr, Pb, Zn, Cu, Mg) of tooth enamel is an increasingly common strategy to reconstruct diet, mobility, ecology and physiology of ancient organisms (Bentley, 2006; Jaouen et al., 2016; Martin et al., 2017; Samuelsen and Potra, 2020). The key prerequisite to such studies is that fossil tissues must preserve biogenic chemical signals without post-depositional contamination or alteration. Rapid (months to years) diagenetic alteration leading to the overwriting of biological signals with the geogenic ones from the depositional environment is well documented for bone and dentin (Keenan and Engel, 2017; Nelson et al., 1986; Reynard and Balter, 2014; Trueman et al., 2004). The main process responsible for the uptake of trace elements in deposited hard tissues is the flow of soil pore-water through the tissue, leading to the dissolution of the smaller crystallites and the redeposition of calcium carbonate onto the larger crystallites (a process known as Ostwald ripening), thus incorporating trace elements present in the pore-water (Trueman et al., 2004). This process is favored by the decay of the organic matrix that opens new spaces for the flow of pore-water. Therefore, the highly mineralized tooth enamel (<1% organic material; Hillson, 2005) is assumed to be resistant to diagenetic alteration (Lee-Thorp and van der Merwe, 1991; MacFadden et al., 2010), especially if appropriate pretreatment is enacted (Wathen et al., 2022). However, a handful of studies have shown that enamel can be

* Corresponding author.
E-mail address: alex.bertacchi@yale.edu (A. Bertacchi).

https://doi.org/10.1016/j.jasrep.2024.104403
Received 13 April 2023; Received in revised form 3 January 2024; Accepted 17 January 2024
Available online 30 January 2024

Table 1
Representative instrument parameters used during LA-MC-ICP-MS data collection.

ESL193 Laser Ablation System		Neptune MC-ICP-MS	
Pattern	Scan line	Plasma power	1270 W
Spot size	65 μm	Sample gas	0.751 L/min
Scan line length	~1200 μm (1.2 mm)	Auxiliary gas	0.85 L/min
Fluence	2.15 J/cm^2	Cool gas	17 L/min
Scan speed	10 μm/sec	Resolution	Low
Repetition rate	20 Hz	Dwell time per channel	~0.1 sec
Carrier gas flow rate	0.5 L/min He	Integration time	~1.0 sec
Gas blank duration	~30 s	Cycle time	~10 s
Ablation duration	~120 s	Cycles/block	12 cycles

Table 2
MTCs calculated from enamel of 56 modern Kenyan mammals. *Provided MTC is the reporting limit because there were no > RL observations.

	n > RL	Max (ppm)	Mean (ppm)	St Dev (ppm)	MTC1 (ppm)	MTC2 (ppm)
Al	56	325.8	55.7	59.5	444.8	174.7
Ca	56	598,740	290,547	122675.6	844091.6	535898.4
Ti	55	249.5	7	33.5	316.5	74
V	53	1.2	0.3	0.3	1.8	0.9
Cr	40	261.8	10.6	45.3	352.4	101.2
Fe	55	1825	185	342.3	2509.6	869.9
Rb	51	1.3	0.2	0.2	1.7	0.6
Sr	56	1036	417	284	1603.6	985
Y	29	1.4	0.2	0.2	1.8	0.6
Ba	56	609.9	60.9	96.4	802.7	253.7
La	29	1.3	0.2	0.3	1.9	0.8
Ce	38	5.8	0.6	1	7.8	2.6
Pr	6	0.2	0.1	0.1	0.4	0.3
Nd	27	0.8	0.2	0.2	1.2	0.6
Sm	4	0.2	0.2	0.1	0.4	0.4
Eu	2	0.1	0.1	0	0.1	0.1
Gd	3	0.2	0.1	0.1	0.4	0.3
Dy	3	0.2	0.1	0.1	0.4	0.3
Ho	0	<RL	NA	NA	0.1*	0.1*
Er	1	0.1	0.1	NA	0.1	0.1
Tm	0	<RL	NA	NA	0.1*	0.1*
Yb	1	0.1	0.1	NA	0.1	0.1
Lu	0	<RL	NA	NA	0.1*	0.1*
Hf	1	0.1	0.1	NA	0.1	0.1
Tl	0	<RL	NA	NA	0.1*	0.1*
Th	7	0.1	0.1	0	0.1	0.1
U	3	0.1	0.1	0	0.1	0.1

diagenetically altered and, critically, this does not appear to be simply a consequence of time spent in the burial environment (Chiaradia et al., 2003; Giovas et al., 2016; Hinz and Kohn, 2010; Kohn et al., 1999). The outermost ~100 μm of enamel in contact with the environment as well as the enamel in direct contact with the dentin are particularly prone to diagenetic alteration (Bourgon et al., 2020; Weber et al., 2021). The implications of these studies are far-reaching because a vast corpus of work rests on the assumption that tooth enamel is resistant to diagenetic transformations and faithfully preserves biogenic elemental and isotopic signals. Similarly, heavy isotope analysis of ostrich eggshell (OES) is an emerging area of archaeometric research for provenience determination and chronometric dating (e.g., Hodgkins et al., 2018; Loewy et al., 2020; Sharp et al., 2019; Stewart et al., 2020). However, OES can be altered through uptake of elements from the burial environment (e.g., uranium; Sharp et al., 2019) and measurements can be affected by the accumulation of microscopic detritus in pore spaces (Loewy et al., 2020). Therefore, developing reliable methods for detecting post-depositional diagenetic alteration to the elemental composition of OES is of critical importance for future studies.

Our approach to developing diagenesis detection methods for enamel and OES was two-fold. First, we sought to calculate Maximum Threshold Concentrations (MTCs) for trace elements measured by Inductively Coupled Plasma-Mass Spectrometry (ICP-MS), directly following Grimstead et al. (2018) and Kamenov et al. (2018), and earlier work by Reynard and Balter (2014). Secondly, we used data collected during strontium isotope ratio analysis by Laser Ablation-Multi Collector (LA-MC)-ICP-MS, the $^{85}Rb/^{88}Sr$ ratio, to determine if this represents a viable additional proxy for diagenesis. The rationale underlying the MTC approach is that by measuring the concentrations of various elements in modern specimens that are ostensibly free of diagenetic alteration, we can generate expectations for the concentrations of these same elements in ancient specimens. Many of these elements are rare in biogenic apatite (or calcite for OES), but common in the burial environment. If these thresholds are exceeded, the specimen has probably taken up geogenic contaminants and may be unsuitable for isotope analysis (Kamenov et al., 2018). Thus, this approach differs from the monitoring of trace element concentrations in fossil enamel alone (i.e., without comparison to a modern reference set) which is already part of some analytical protocols (e.g., Kowalik et al., 2020, 2023; Kubat et al., 2023, Rey et al., 2022).

The premise of the rubidium-strontium ratio approach is as follows. While strontium readily substitutes for calcium in biogenic apatite and calcite due to their similar ionic radii (Pollard et al., 2007), rubidium similarly substitutes for potassium. In a Ca-dominated matrix like enamel or OES, rubidium concentrations are thus expected to be small in comparison to strontium. Isobaric interference by calcium and rubidium during radiogenic strontium ratio measurement is a routinely encountered issue but sample preparation (ion chromatography) and data processing (interference corrections including considerations for instrumental mass fractionation) procedures take this into account (Horsky et al., 2016; Irrgeher et al., 2013). Mass-to-charge ratio (m/z) 85 is typically monitored in order to use the measured ^{85}Rb signal and the natural $^{85}Rb/^{87}Rb$ ratio to correct for interference on m/z 87 (e.g., Copeland et al., 2016). M/z 88, the most abundant isotope of strontium, is measured as an indicator signal strength during instrument tuning and data collection. In light of the expected low concentration of rubidium relative to strontium in enamel and OES, and the already routine collection of m/z 85 and 88 data, it occurred to us that elevated $^{85}Rb/^{88}Sr$ ratios in archaeological specimens could serve as an additional proxy for diagenesis. This approach is applicable to LA-MC-ICP-MS of solid samples that have not been subjected to ion chromatography to remove calcium, rubidium, barium and other interfering elements prior to analysis, or to solution MC-ICP-MS samples prior to ion chromatography. If effective, the $^{85}Rb/^{88}Sr$ diagenesis proxy has the potential to permit identification of post-depositional alteration without separate solution ICP-MS or LA-ICP-MS analysis specifically for this purpose. For samples measured by ICP-MS, we calculated whole element Rb/Sr instead, following the same logic.

2. Materials and methods

2.1. Measuring elemental concentrations in modern enamel

Our modern sample of ostensibly unaltered enamel includes 56 individual mammals from several localities in southern Kenya, housed at the Yale Peabody Museum of Natural History (New Haven, CT, USA). The sample (see Supplementary Online Materials [SOM] 1) includes 6 dietary categories (grazers = 15, browsers = 26, mixed feeders = 4, frugivorous bovids = 1 [hereafter grouped with the browsers], carnivores = 6, omnivorous suids = 4; bovid dietary categories after Gagnon and Chew, 2000, as amended by Cerling et al., 2003; Sponheimer et al., 2003) and 25 different species. We hypothesized that dietary category might influence trace element concentrations in enamel (Balter et al., 2002, 2012; Kubat et al., 2023).

Teeth were drilled along the crown using diamond-coated tungsten

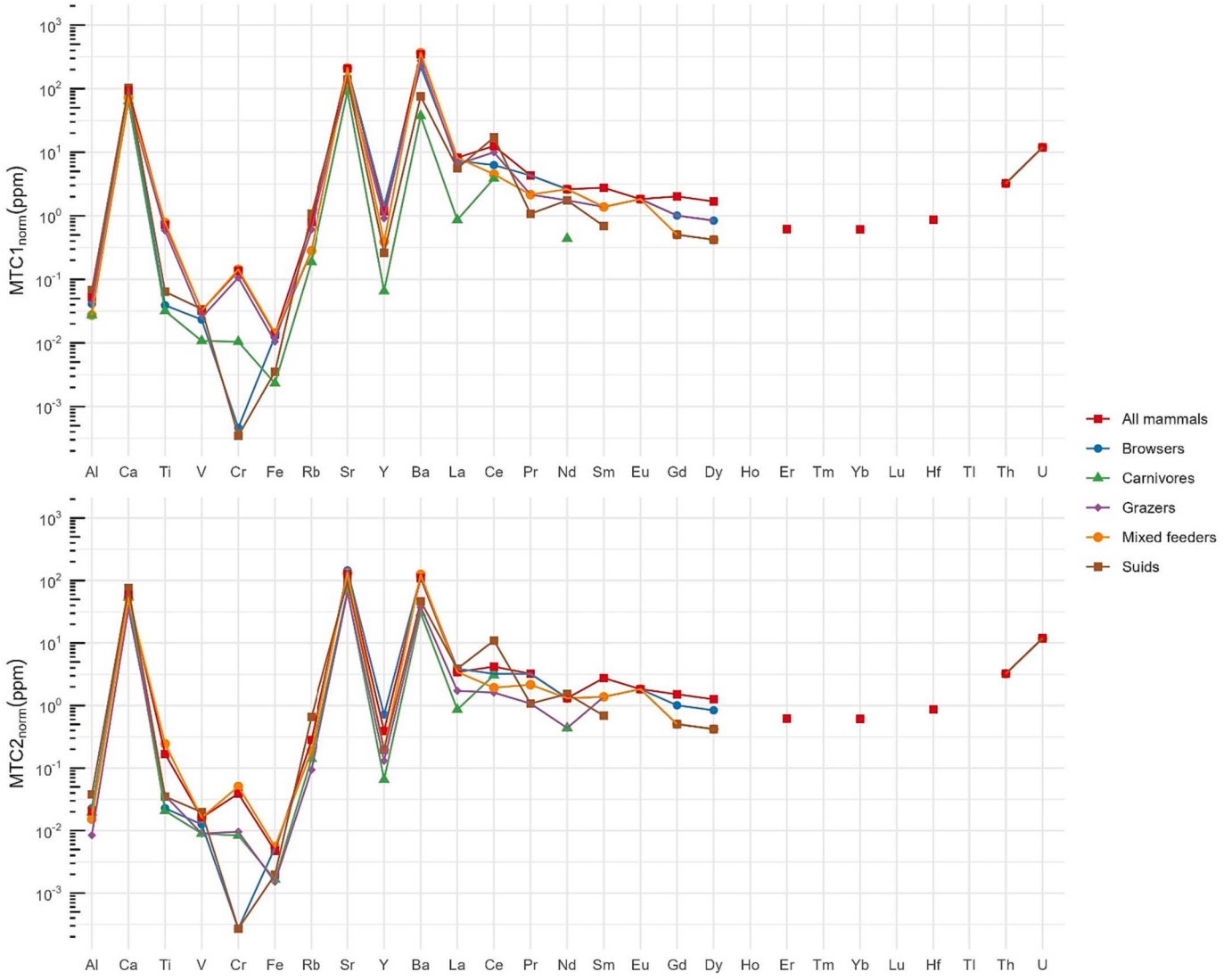

Fig. 1. MTC1 and MTC2 calculated for enamel from modern Kenyan mammals (ThermoScientific Element XR measurements). Missing data points denote elements for which no MTCs could be calculated because all measurements were below reporting limits. Elemental abundances are normalized to CI chondrite. Note that the y-axis is base10 logarithmic. The tight values and small variation in Ca and Sr are driven by stochiometric constraints in carbonate-substituted hydroxyapatite.

burrs mounted on a Manipro™ tool. Before each sampling event, the burr was immersed in 0.1 M HCl for a few seconds to remove residues from previous samples, then sonicated in ultrapure water. Here and throughout, when we refer to ultrapure water, we refer to Milli-Q Direct Type 1 water with >18.0 MΩ•cm resistivity. At least 2 mg of powdered enamel (free of any dentine) from each sample were transferred to an acid-cleaned PFA beaker (Savillex™), capped and dissolved overnight in 1 ml 6.2 M double distilled HCl at 120 °C. After the addition of two drops of 30% H_2O_2 the samples were dried down and acidified in 1.5 ml 5% HNO_3 spiked with indium for instrumental normalization. Here and throughout, when we refer to HNO_3 we refer to acid that has been double distilled in-house. We measured several isotopes (*m/z* ratios; see SOM 2) on a magnetic sector ThermoScientific Element XR ICP-MS at the Yale Metal Geochemistry Center and hereafter report whole element concentrations of Al, Ca, Ti, V, Cr, Fe, Rb, Sr, Y, Ba, La, Ce, Pr, Nd, Sm, Eu, Gd, Dy, Ho, Er, Tm, Yb, Lu, Hf, Tl, Th and U. Since the goal is to measure trace element uptake, samples did not undergo ion chromatography (the same applies to OES below). Calibration is based on a series of dilutions of a primary in-house carbonate reference material. Quality control/quality assurance was maintained through analyses of secondary reference materials BHVO-2, SBC-1, COQ-1 and an in-house matrix-matched modern cow (*Bos taurus*) enamel reference material.

2.1.1. Measuring elemental concentrations in modern ostrich eggshell (OES)

Our sample of modern ostrich eggshell specimens is composed of three assemblages: 20 eggshells collected as fragments from abandoned wild ostrich nests in the Namibian Kalahari Desert, 12 eggs collected as fragments from abandoned wild nests on the south coast of South Africa, and 3 eggs provided as large fragments by the Rooster Cogburn Ostrich Ranch in Picacho, Arizona, USA. All specimens were from the ostrich subspecies *Struthio camelus australis* (Gurney 1868). These assemblages were acquired as part of a separate method development project about *in situ* radiogenic strontium isotope ratio analysis of OES using LA-MC-ICP-MS and were repurposed after that work was completed.

Data collection for the first approach, measurement of multiple trace elements in OES to calculate MTCs, was done using solution quadrupole ICP-MS with a ThermoScientific iCAP Q instrument at the Arizona State University (ASU) Metals, Environmental, and Terrestrial Analytical Laboratory (METAL). Initial sample preparation was undertaken in the School of Human Evolution and Social Change (SHESC) Archaeological Chemistry Laboratory. Each OES specimen for analysis was manually cleaned of organic debris (e.g., soil, plant matter, and shell membrane, if present) and subjected to two 30-minute periods of ultrasonic cleaning in acid-cleaned glassware filled with ultrapure water. Water in each

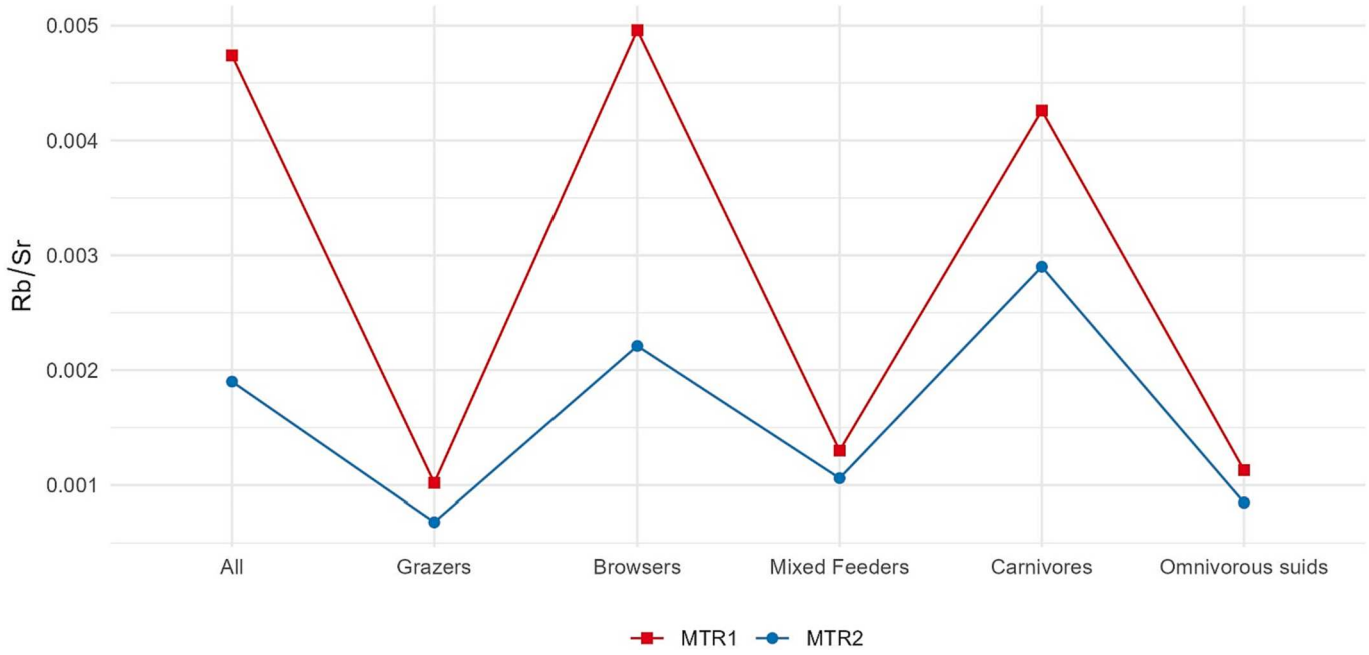

Fig. 2. Whole element Rb/Sr in enamel from modern Kenyan mammals (ThermoScientific Element XR measurements).

Table 3
Elemental MTCs calculated from 20 wild-collected Namibian Kalahari ostrich eggshells (40 sub-samples total). *Provided MTC is the reporting limit because there were no > RL observation.

Element	n > RL	Max (ppm)	Mean (ppm)	St Dev (ppm)	MTC1 (ppm)	MTC2 (ppm)
V	2	0.1	0.08	0.01	0.12	0.11
Mn	10	45	17	14	74	46
Fe	40	67	9	12	92	34
Ce	5	0.23	0.11	0.07	0.37	0.24
Nd	2	0.1	0.1	0	0.1	0.1
Dy	1	0.01	0.01	0	0.01	0.01
Yb	0	<RL	<RL	NA	0.05*	0.05*
Th	24	0.52	0.04	0.1	0.72	0.24
U	6	0.051	0.025	0.016	0.083	0.057

Table 4
Elemental MTCs calculated from 12 wild-collected South African ostrich eggshells (24 sub-samples total). *Provided MTC is the reporting limit because there were no > RL observations.

Element	n > RL	Maximum (ppm)	Mean (ppm)	St Dev (ppm)	MTC1 (ppm)	MTC2 (ppm)
V	1	0.06	0.06	0	0.06	0.06
Mn	0	<RL	<RL	NA	5*	5*
Fe	24	46	8	10	66	27
La	2	0.06	0.05	0.01	0.07	0.06
Ce	3	0.1	0.09	0.01	0.11	0.1
Pr	2	0.013	0.011	0.002	0.016	0.015
Nd	0	<RL	<RL	NA	0.1*	0.1*
Sm	3	0.01	0.01	0	0.01	0.01
Eu	0	<RL	<RL	NA	0.005*	0.005*
Gd	3	0.01	0.01	0	0.01	0.01
Tb	0	<RL	<RL	NA	0.005*	0.005*
Dy	2	0.01	0.01	0	0.01	0.01
Ho	0	<RL	<RL	NA	0.005*	0.005*
Er	0	<RL	<RL	NA	0.05*	0.05*
Tm	0	<RL	<RL	NA	0.005*	0.005*
Yb	0	<RL	<RL	NA	0.05*	0.05*
Lu	0	<RL	<RL	NA	0.005*	0.005*
Hf	24	0.49	0.05	0.1	0.68	0.24
Pb	7	0.17	0.08	0.04	0.25	0.16
Th	3	0.01	0.01	0	0.02	0.01
U	6	0.021	0.013	0.006	0.033	0.025

vessel was replaced between consecutive cleaning periods and OES specimens were then air dried in a 40 °C drying oven. After drying, material for digestion and analysis was removed separately from the inner and outer surface of each shell specimen using a diamond-coated burr mounted on a Dremel™ rotary tool. Different burrs were used for the inner and outer surface and all burrs were sonicated in ultrapure water followed by a final methanol rinse between uses. For the outer surface, we took care to avoid drilling in or near shell pores visible to the unaided eye. For the inner surface, the specimen was abraded indiscriminately. Between 50 and 90 mg of powdered shell were collected from each specimen surface.

Each powder sample was digested in 4 ml 2 M HNO_3 in acid-cleaned, capped, PFA beakers (Savillex™) at 120 °C for four hours to yield a 4 ml stock solution. Shell sample and reagent mass were recorded to 0.0001 g and used to calculate a dilution factor for the stock solution. A 0.53 ml aliquot of stock solution was pipetted into a metal-free centrifuge tube and diluted to 15 ml using 0.32 M HNO_3. Aliquot and acid mass were again recorded and used to calculate a second dilution factor. The final, overall dilution factor for each specimen ranged from 4400 to 5400×.

Each dilute aliquot was analyzed for trace elements using a ThermoScientific iCAP Q (single quadrupole) ICP-MS in Kinetic Energy Discrimination (helium KED) mode. This configuration attenuates the high-intensity calcium signal of the matrix and mitigates polyatomic interferences. Prior to beginning analysis of OES solutions, a 500 ppm calcium solution was run for ~30 min to condition the instrument and mitigate fluctuations in plasma suppression during the subsequent analyses. Calibration used a multi-element external calibration solution formulated from single element, NIST-traceable, solution reference materials spiked with calcium to matrix-match the OES solutions. Spikes for normalization included ^{45}Sc, ^{72}Ge, ^{89}Y, ^{115}In, and ^{209}Bi and were introduced online during analysis. These methods are common to all three OES assemblages. However, the analytes measured differ because this part of the project evolved from routine quality control measurements undertaken as part of the ASU METAL standard operating procedure for $^{87}Sr/^{86}Sr$ measurement. For analyte lists see SOM 3. Hereafter, concentrations are reported for whole elements. External

Table 5
Elemental MTCs calculated from 3 farm-raised Arizona (USA) ostrich eggshells (6 sub-samples total). *Provided MTC is the reporting limit because there were no > RL observations.

Element	n > RL	Maximum (ppm)	Mean (ppm)	St Dev (ppm)	MTC1 (ppm)	MTC2 (ppm)
V	0	<RL	<RL	NA	0.05*	0.05*
Mn	2	10	8	3	15	13
Fe	6	17	10.5	3	23	17
La	0	<RL	<RL	NA	0.05*	0.05*
Ce	2	0.07	0.06	0.01	0.09	0.08
Pr	1	0.005	0.005	0	0.005	0.005
Nd	0	<RL	<RL	NA	0.1*	0.1*
Sm	0	<RL	<RL	NA	0.01*	0.01*
Eu	0	<RL	<RL	NA	0.005*	0.005*
Gd	0	<RL	<RL	NA	0.01*	0.01*
Tb	0	<RL	<RL	NA	0.005*	0.005*
Dy	0	<RL	<RL	NA	0.01*	0.01*
Ho	0	<RL	<RL	NA	0.005*	0.005*
Er	0	<RL	<RL	NA	0.05*	0.05*
Tm	0	<RL	<RL	NA	0.005*	0.005*
Yb	0	<RL	<RL	NA	0.05*	0.05*
Lu	0	<RL	<RL	NA	0.005*	0.005*
Hf	6	0.19	0.09	0.05	0.3	0.2
Pb	6	0.21	0.13	0.05	0.31	0.22
Th	6	0.06	0.03	0.02	0.1	0.07
U	6	0.031	0.01	0.009	0.05	0.03

calibration and internal standardization (normalization) were carried out using the ThermoScientific Qtegra software.

2.1.2. Measuring Rb/Sr ratios by LA-MC-ICP-MS in modern OES

In all three OES assemblages, Rb/Sr was calculated from the elemental concentrations measured in dilute aliquots by quadrupole ICP-MS as described above (see Section 2.1.1). Additionally, the isotopic signal intensity ratio $^{85}Rb/^{88}Sr$ was measured by LA-MC-ICP-MS only for the Namibian modern OES assemblage. After washing and drying (see Section 2.1.1), one fragment per shell was mounted with double-sided pressure sensitive adhesive tape on a glass microscope slide. Laser ablation was carried out with an Elemental Scientific NWR193UC (i.e., ESL193) 193 nm Excimer laser ablation system coupled to a Thermo-Finnigan Neptune MC-ICP-MS. Prior to undertaking this project, optimal laser parameters were determined through several measurements of silicate glass (e.g., NIST SRM 610 and 612), matrix-matched calcium carbonate reference materials including USGS MACS-3 (Weber et al., 2018), NanoSr (Weber et al., 2020), and JCp-1-NP (Jochum et al., 2019), as well as additional modern OES samples not reported in this manuscript. These reference materials were not employed as calibrants for data reduction; rather, they only were used to determine the most effective laser settings for ablating OES and measuring Rb and Sr signals with low instrumental uncertainty. Ultimately, ablation and measurement of OES specimens were carried out using the parameters in Table 1. Processing of raw signal intensity data was carried out using the Iolite v4 (Elemental Scientific Lasers) software application, with the Baseline Subtract data reduction scheme. This simply calculates the average pre-ablation "gas blank" signal intensity for each analyte and subtracts it from average signal intensity calculated during the ablation period. The $^{85}Rb/^{88}Sr$ signal intensity ratios from LA-MC-ICP-MS reported here are thus only corrected for background signal and not for mass fractionation.

2.2. Calculation of maximum threshold concentrations and ratios

In the following section we refer to two variations of the maximum threshold concentration and the maximum threshold ratio (MTR). As mentioned above, MTRs are most relevant to LA analyses of solid samples, but are applicable to solution samples as well. MTC1 and MTR1 are calculated with the approach used by Kamenov et al. (2018): for each element the threshold is defined as the maximum value (elemental concentration or ratio) measured in a set of modern, unaltered samples, plus two times the standard deviation in the applicable data set:

$$MTC(orMTR)1 = ModernMax + 2xModernSTDEV$$

Additionally, we propose the use of a more conservative threshold: MTC2 and MTR2.

$$MTC(orMTR)2 = ModernMean + 2xModernSTDEV$$

By replacing the maximum concentration or ratio observed in the data set with the mean concentration or ratio, the resulting threshold value is based on a measure of central tendency rather than a single, potentially outlier, datum. We recommend the calculation of both thresholds to highlight cases where substantial disparities exist and require further investigation.

For elemental MTCs, calculation of the threshold sometimes required the exclusion of individual results below the applicable Limit of Detection (LOD). LODs vary between instruments and even between analytical sessions with the same instruments. Therefore, to facilitate comparisons we adopt a more conservative Reporting Limit (RL), specified in SOM 2 and 3. MTCs were calculated using only >RL concentrations (counts are included in the tables). In all figures, MTCs have been normalized by dividing the concentration of each element by the concentration of the corresponding element in the CI chondrite (Lodders, 2003) to account for the natural abundance of different elements in the environment and mitigate the confounding effect of the Oddo-Harkins rule (*i.e.*, higher abundance of elements with even number of protons; Harkins, 1917).

3. Results

3.1. MTCs and MTRs in modern enamel

Enamel MTCs determined from modern Kenyan mammals are reported in Table 2 and Fig. 1 (complete results and descriptive statistics in SOM 2). A single sample (ABM 38) is an outlier with very low concentrations of all measured elements. Calcium content averages ~29% by weight (~33.6% in the cow enamel standard), which is within the ~20–40% range reported for miscellaneous non-human mammals (Buddhachat et al., 2016; de Dios Teruel et al., 2015; Sato et al., 1995). No measurements were above the applicable RL for the elements holmium, thulium, lutetium and thallium. In several cases, MTC1s are one order of magnitude higher than the more conservative MTC2s. When

Table 6
Summary of the Rb/Sr measurements.

	Enamel	Pooled OES		Inner OES		Outer OES	
	Rb/Sr	$^{85}Rb/^{88}Sr$	Rb/Sr	$^{85}Rb/^{88}Sr$	Rb/Sr	$^{85}Rb/^{88}Sr$	Rb/Sr
n > RL	51	28	20	14	6	14	14
Max	0.0034	0.0030	0.0020	0.0004	0.0014	0.0030	0.0020
Mean	0.0006	0.0005	0.0005	0.0001	0.0003	0.0009	0.0006
St Dev	0.0006	0.0007	0.0006	0.0001	0.0005	0.0008	0.0006
MTR1	0.0047	0.0044	0.0031	0.0006	0.0024	0.0045	0.0031
MTR2	0.0019	0.0019	0.0016	0.0003	0.0013	0.0025	0.0017

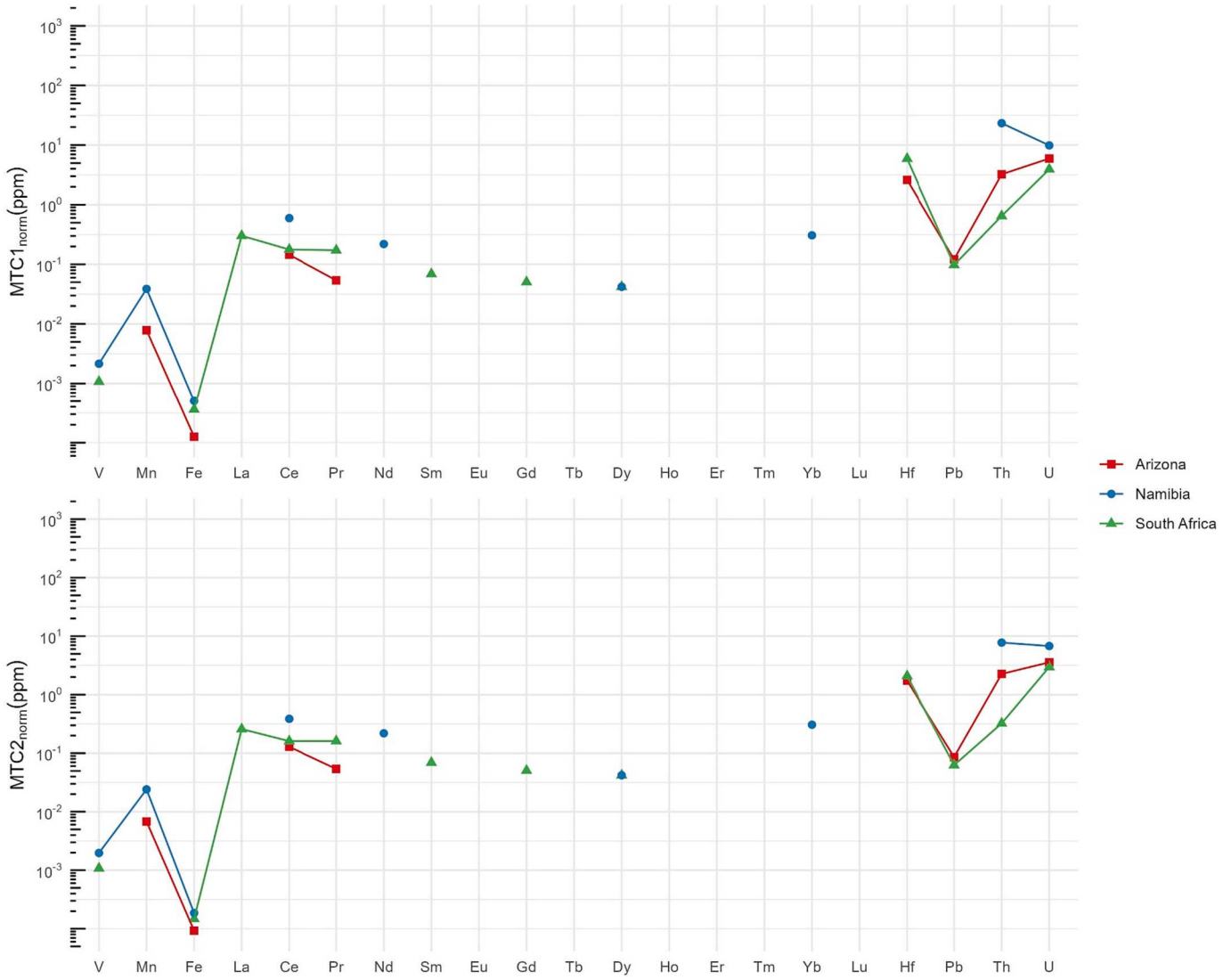

Fig. 3. MTC1 and MTC2 calculated for modern OES from Arizona, Namibia and South Africa (ThermoScientific iCAP ICP-MS measurements). Missing data points denote elements for which no MTCs could be calculated because all measurements were below reporting limit or the corresponding analyte was not measured. Elemental abundances are normalized to the CI chondrite. Note that the analyzed elements are the same for the South Africa and Arizona data sets, while the Namibia Kalahari data set only includes nine of the 21 elements measured for the other data sets.

calculating MTCs for specific dietary categories, many elements are found in concentrations below the RL and therefore these more specific MTCs might be overly conservative until larger samples of modern enamel are included. Comparisons between dietary groups and with the pooled sample of modern Kenyan mammals clearly shows that elemental concentrations follow similar patterns across groups, with only minor differences in absolute concentrations and virtually no differences in trends (Fig. 1). The only highly variable element is chromium, which is elevated in browsers and might signal exposure to industrial pollutants (cf. Kamenov et al., 2018). As expected, Rb/Sr is consistently low at 10e−4 and 10e−5 (Fig. 2, Table 6).

3.2. MTCs in modern OES

We report elemental MTCs for the three modern OES assemblages in Tables 3–5 and Fig. 3 below (complete results and descriptive statistics in SOM 3). In the tables, we pool inner and outer shell measurements (reported separately in SOM 3). In the Namibian Kalahari assemblage (Table 3), most elements have a low fraction of significant (>RL) observations; consequently, the MTCs for these elements should be considered informational only. Only two measured elements in the Kalahari data set, iron and thorium, have greater than 50 % associated >RL observations.

The South African and Arizona data sets, which were generated after the Kalahari data set, expanded the list of analyzed analytes from nine to 21, predominantly through the addition of further Rare Earth Elements (REE). For the South African OES data set (Table 4), iron and hafnium have MTCs calculated from 100% >RL observations. All other elements yielded less than 50% >RL observations. Thorium only yielded 3 >RL observations (12.5%), in contrast to the Kalahari data set in which thorium yielded 60% >RL observations. Manganese is an additional contrast, with no >RL observations for South Africa versus 25% for the Kalahari data set. The Arizona OES data set (Table 5) is very small but can be used as a comparison to the wild-collected OES data sets. Consistently with the other assemblages, the Arizona OES showed no or very few >RL observations for most of the REEs measured. Iron, hafnium, lead, thorium and uranium yielded 100% >RL observations. In all data sets, iron is the element with the most >RL observations. Hafnium exhibited 100% >RL observations in the South African and Arizona data sets but was not measured in the Namibian assemblage. The proportion of >RL observations for thorium and uranium is inconsistent across data sets.

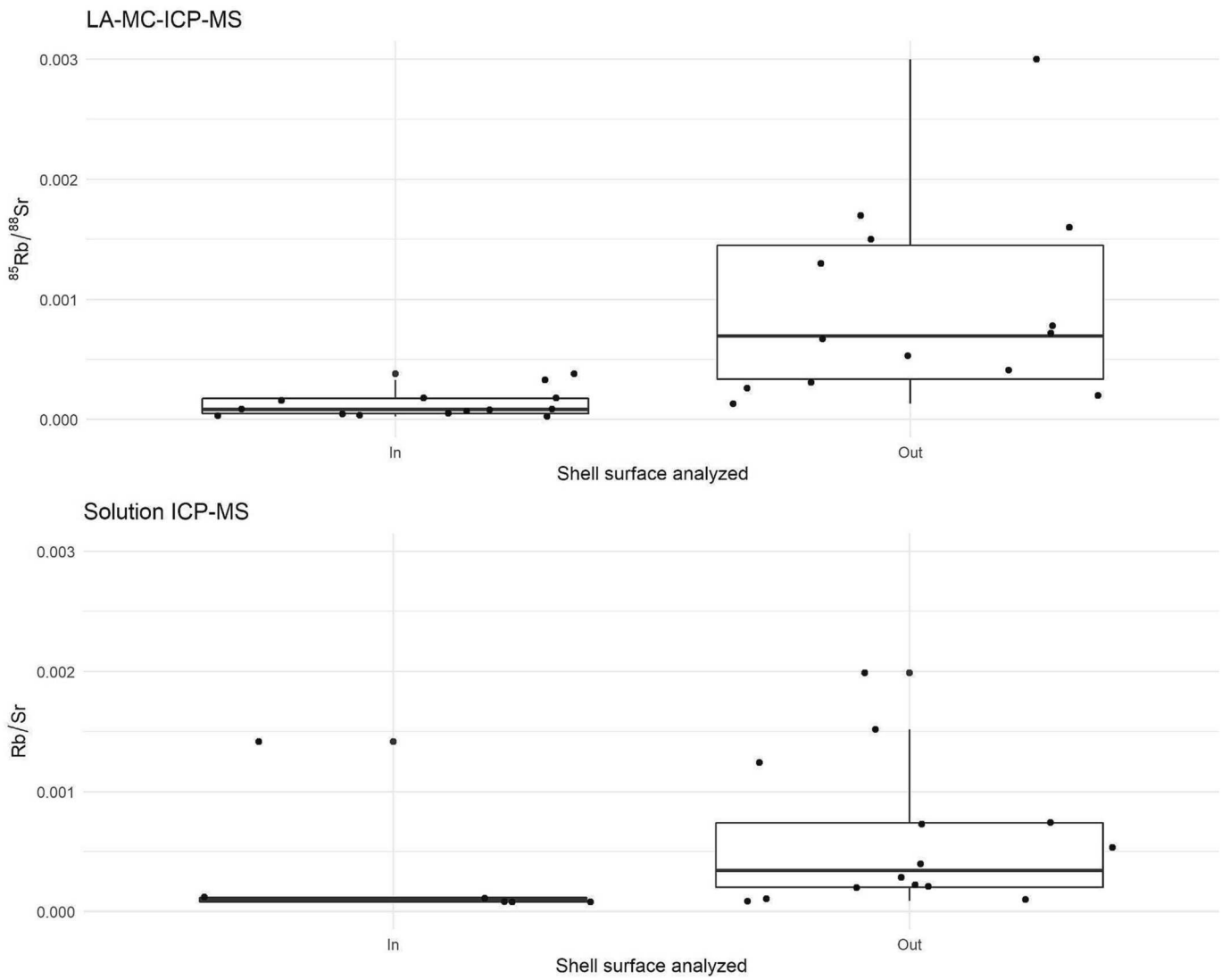

Fig. 4. $^{85}Rb/^{88}Sr$ and Rb/Sr measured on the inner and outer surfaces of the same ostrich eggshell fragments from Namibia by LA-MC-ICP-MS (ThermoFinnigan Neptune) and solution ICP-MS (ThermoScientific iCAP), respectively. Note that eight of the inner shell solution measurements were below detection level.

The difference between MTC1 and MTC2 varies across measured elements, from no difference to MTC1 being three times higher than MTC2. When comparing MTCs calculated for the inside and the outside of the OES (SOM 3), there is no pattern in which sub-sample type exhibits higher concentrations of trace elements.

In Fig. 4 and Table 6, we compare whole element Rb/Sr measured by solution ICP-MS and $^{85}Rb/^{88}Sr$ measured by LA-MC-ICP-MS for the Namibian OES assemblage (full results in SOM 3). As noted in the methods, the solution ICP-MS measurements are in the form of externally calibrated elemental concentrations calculated from the intensity signal for m/z 85 and 88, while the LA-MC-ICP-MS results are background corrected signal intensity ratios for m/z 85 and 88. Despite being an imperfect comparison, we chose to present the results in this format because they represent the way such data are likely to be collected in the context of $^{87}Sr/^{86}Sr$ analyses in an archaeological study.

Both solution and laser ablation approaches yield similar results, although eight inner shell measurements by solution ICP-MS were below RL. Both techniques also yielded large standard deviations caused by outliers. MTR2 is about half of MTR1 in each sub-sample and in the pooled sample.

4. Discussion

This study implemented Kamenov and colleagues' (2018) MTC1 (modern max + 2 * STDEV) approach to a taxonomically diverse assemblage. We also explored the calculation of a more conservative MTC2 (modern mean + 2 * STDEV) which should not inevitably increase with increasing size of the modern sample from which the MTC is calculated. Each type of MTC has its strengths and weaknesses and we suggest considering both. MTC2 is less susceptible to outliers, but is limited by measurements below RL, while MTC1 is minimally affected by the latter but highly susceptible to outliers. Which MTC is best suited for any particular study also depends on how reasonable is the assumption that all modern reference specimens are in fact free of contaminants (e.g., industrial pollutants, museum conservation products). Furthermore, we developed MTCs specific to certain dietary categories and taxonomic groups, although at present their use is limited by small sample sizes.

Overall, our results suggest that MTCs are consistent across taxa at a single locality (Fig. 1). Therefore, we propose that, when possible, researchers measuring heavy isotope ratios in archaeological enamel or eggshell should consider analyzing modern specimens from the same locality to provide trace element threshold values for unaltered tissues.

Locality-specific trace element baselines have been observed in the

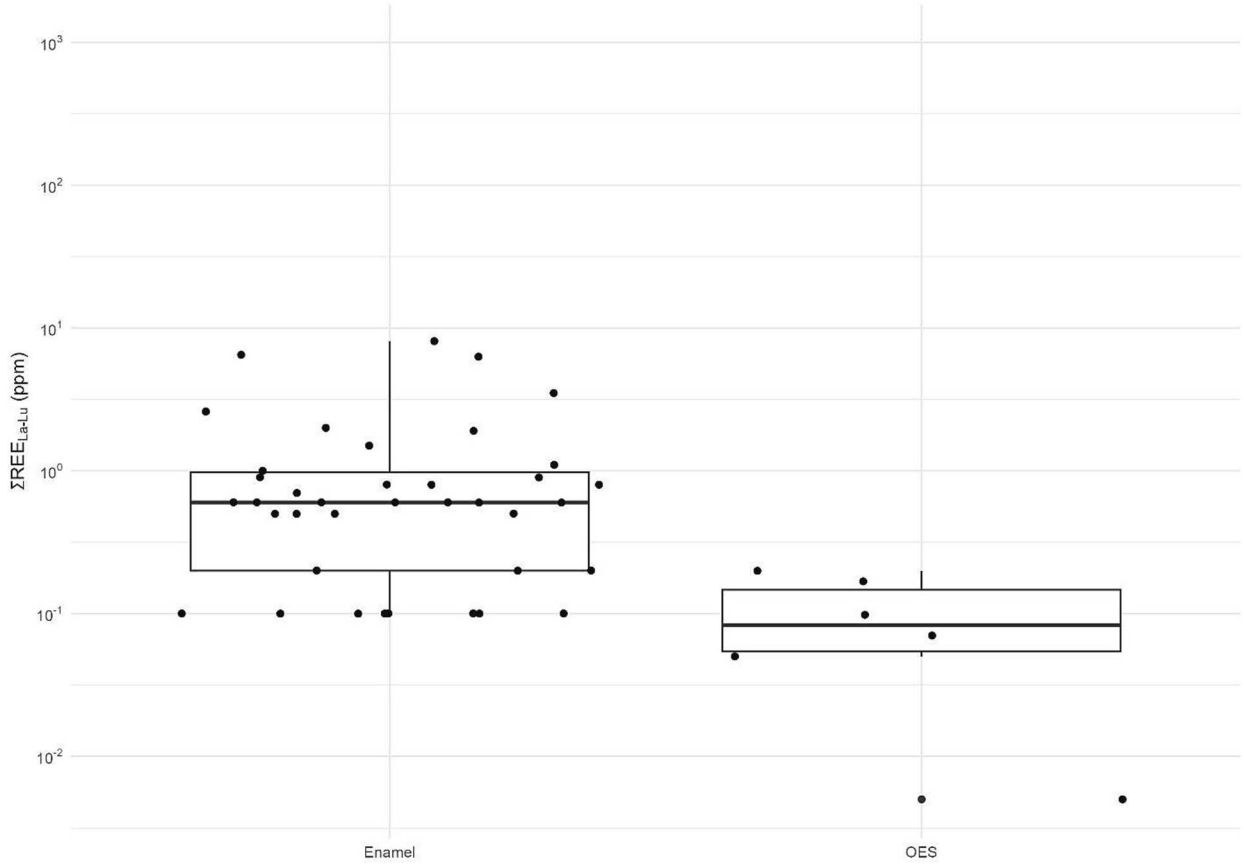

Fig. 5. ΣREE$_{La-Lu}$ (ppm) in modern enamel and OES. Specimens that yielded no observations > RL are not plotted.

fossil record before. For instance, MacFadden et al. (2010) observed statistically distinct REE baselines across Late Cenozoic fossil sites in Florida and proposed that the locally-distinct chemistry of pore-waters had an effect on the uptake of REE in fossil specimens. Our results suggest that differences across localities may be recorded *in-vivo* as well. The modern sample need not be of the same taxa analyzed, which may be impractical or require special permits for studies that deal with wild taxa. We argue that it is desirable to develop more taxon-specific MTCs, but also maintain that our preliminary data suggest that understanding the spatial variability in trace element baselines has a larger impact than inter-taxonomic variation in trace element uptake.

REE (i.e., the lanthanides: lanthanum [Z = 57] to lutetium [Z = 71]; as well as scandium [Z = 21] and yttrium [Z = 39]) are particularly scarce in biological hard tissues *in vivo*, but are quickly up-taken after deposition (Trueman et al., 2004). For this reason, they are considered indicators of diagenetic alteration (e.g., MacFadden et al., 2010, Kamenov et al., 2018). Our results support this, especially for the middle and heavy REE (from samarium [Z = 62] to lutetium), whose concentrations in modern specimens are often below RL. High concentrations of these elements in fossil specimens may signal important diagenetic alteration even in absence of formal MTCs. For heavily altered fossil bone, ΣREE are reported in the range of 10e2–10e5 ppm (e.g., Kocsis et al., 2010). In our set, ΣREE$_{La-Lu}$ did not exceed 10e1 ppm for enamel and 10e0 ppm for OES (Fig. 5). However, available case studies suggest that measuring multiple elements *in addition* to REE is warranted. For instance, Gatti et al. (2022) observed that a diagenetically altered bone had unusually low REE concentrations, perhaps because the burial environment was depleted in those, but the altered status of the specimen was still reflected in high concentrations of uranium and strontium. In some cases spikes in trace element concentrations in fossil enamel are not reflected in changes in $^{87}Sr/^{86}Sr$ (e.g., up to 1.3 ppm uranium in Kowalik et al., 2023). Therefore, exclusion of individual samples needs to be carefully considered on a case-by-case basis.

Therefore, we argue that several trace elements should be measured in archaeological specimens prior to heavy isotope analysis even in the absence of formal MTCs. Thus, the specimens can be screened for diagenetic alteration *post-hoc* once formal MTCs become available. One further reason to build site-level databases of trace element concentrations is that the preservation of the mineral fraction of skeletal elements is a viable proxy for the preservation of the organic fraction (Gatti et al., 2022). This is now relevant to enamel as mineral-bound nitrogen is measured in fossil material (Leichliter et al., 2021).

MTRs in enamel and OES are comparably low at 10e−4, suggesting that these levels may be typical of unaltered, biogenic hard tissues. These values are consistent with, and stricter than, conventional cutoffs adopted in the literature (e.g., Rb/Sr 0.02 in Irrgeher et al., 2016). The concentrations of strontium and rubidium should however be considered, otherwise a sample with low biogenic strontium may be misinterpreted as an outlier with high diagenetic rubidium. Concentrations of both strontium and rubidium relative to calcium vary with trophic level and feeding strategy through biopurification (Balter et al., 2002, 2012; Kubat et al., 2023), but we observe unexpected highly consistent Rb/Sr across dietary categories in the enamel set (Fig. 2). MTRs measured in OES show greater dispersion and maximum values when measured in the outer shell than in the inner shell. One interpretation is that despite the premise that modern OES is unlikely to have been affected by chemical exchange with the environment after the eggs were laid, the outer surface has been impacted by diagenesis before the specimens were collected for study. This may be due to the outer shell having been in contact with soil immediately after the egg was laid, providing greater opportunity for chemical exchange relative to the inner shell. Additionally, the inner shell is covered by a membrane that may have shielded the calcium carbonate from direct contact with soil and other sources of rubidium after the egg hatched. It cannot be

discounted, however, that a process occurring during eggshell formation could have led to a greater biogenic rubidium concentration in the outer versus the inner shell. It seems therefore appropriate to generate MTRs (and MTCs) specific to the outer and the inner aspects of OES. Given our limited sample, it is not clear whether the method used to generate the reference set (solution ICP-MS vs. LA-MC-ICP-MS) has an ultimate impact on the applicability of the reference set, but the fact that several solution ICP-MS measurements were below detection limit warrants caution. A final factor to consider is the magnitude of sample and reference material dilution, which affects the LOD and should therefore be appropriately reported. Otherwise, differences across localities studied by different laboratories could be erroneously interpreted as baseline differences, while in reality they are artefacts driven by systematic differences in the way samples were diluted.

5. Conclusions

In this exploratory study, we assessed typical biogenic values for unaltered enamel and OES to determine markers of diagenetic alteration for use in isotopic analyses. We reached the following conclusions:

1) Based on the OES assemblages we conclude that trace element concentrations vary depending on the provenience of the specimen; therefore, reference sets should be locality-specific. This is likely true for enamel as well. Taxon-specific reference sets, while desirable, are of secondary importance.
2) In absence of formal MTCs, ΣREE in the order of 10e1 may serve *tentatively* as a cutoff for unaltered enamel and OES if other diagenetic markers (e.g., uranium) are also low.
3) MTRs in the order of 10e−4 seem typical of unaltered enamel and OES. For OES, it is appropriate to generate reference sets specific to the aspect (inner or outer) being measured.

CRediT authorship contribution statement

Alex Bertacchi: Conceptualization, Data curation, Formal analysis, Funding acquisition, Investigation, Methodology, Resources, Visualization, Writing – original draft, Writing – review & editing. **Andrew M. Zipkin:** Conceptualization, Data curation, Formal analysis, Funding acquisition, Investigation, Methodology, Resources, Visualization, Writing – original draft, Writing – review & editing. **Julia Giblin:** Supervision, Writing – review & editing. **Gwyneth Gordon:** Writing – review & editing. **Tyler Goepfert:** Writing – review & editing. **Dan Asael:** Methodology, Writing – review & editing. **Kelly J. Knudson:** Resources, Writing – review & editing.

The authors declare that they have no known competing financial interests or personal relationships that could have appeared to influence the work reported in this paper.

Data availability

All relevant data is included in the Supplementary Materials.

Acknowledgements

AB thanks Eric Sargis and Kristof Zyskowski (access to modern mammals from the Yale Peabody Museum), Noah Planavsky (access to the Yale Metal Geochemistry Center), Boriana Kalderon-Asael (assistance during measurement of trace elements in modern enamel), Brad Erkkila and Jonas Karosas (access to the Yale Analytical and Stable Isotope Center). AB was partly supported by a Yale Institute of Biospheric Studies (YIBS) Graduate Research Grant. We acknowledge the use of METAL (Metals, Environmental, and Terrestrial Analytical Laboratory) facilities within the Eyring Materials Center at Arizona State University supported in part by NNCI-ECCS-1542160. Laboratory work by AZ was supported by US National Science Foundation Award BCS-2018010 (Wiessner, Zipkin, and Kinahan) and Wenner-Gren Foundation Grant 9801(Zipkin).

Appendix A. Supplementary material

Supplementary data to this article can be found online at https://doi.org/10.1016/j.jasrep.2024.104403.

References

Balter, V., Bocherens, H., Person, A., Labourdette, N., Renard, M., Vandermeersch, B., 2002. Ecological and physiological variability of Sr/Ca and Ba/Ca in mammals of West European mid-Würmian food webs. Palaeogeogr. Palaeoclimatol. Palaeoecol. 186 (1–2), 127–143.

Balter, V., Braga, J., Télouk, P., Thackeray, J.F., 2012. Evidence for dietary change but not landscape use in South African early hominins. Nature 489 (7417), 558–560.

Bentley, A.R., 2006. Strontium isotopes from the Earth to the Archaeological skeleton: a review. J. Archaeol. Method Theory 13 (3), 135–187. https://doi.org/10.1007/s10816-006-9009-x.

Bourgon, N., Jaouen, K., Bacon, A.-M., Jochum, K.P., Dufour, E., Duringer, P., et al., 2020. Zinc isotopes in Late Pleistocene fossil teeth from a Southeast Asian cave setting preserve paleodietary information. Proc. Natl. Acad. Sci. 117 (9), 4675–4681. https://doi.org/10.1073/pnas.1911744117.

Buddhachat, K., Klinhom, S., Siengdee, P., Brown, J.L., Nomsiri, R., Kaewmong, P., Nganvongpanit, K., 2016. Elemental analysis of bone, teeth, horn and antler in different animal species using non-invasive handheld X-ray fluorescence. PLoS One 11 (5), e0155458.

Cerling, T.E., Harris, J.M., Passey, B.H., 2003. Diets of East African Bovidae Based on Stable Isotope Analysis. J. Mammal. 84 (2), 456–470. https://doi.org/10.1644/1545-1542(2003)084<0456:DOEABB>2.0.CO;2.

Chiaradia, M., Gallay, A., Todt, W., 2003. Different contamination styles of prehistoric human teeth at a Swiss necropolis (Sion, Valais) inferred from lead and strontium isotopes. Appl. Geochem. 18 (3), 353–370.

Copeland, S.R., Cawthra, H.C., Fisher, E.C., Lee-Thorp, J.A., Cowling, R.M., le Roux, P.J., et al., 2016. Strontium isotope investigation of ungulate movement patterns on the Pleistocene Paleo-Agulhas Plain of the Greater Cape Floristic Region, South Africa. Quat. Sci. Rev. 141, 65–84. https://doi.org/10.1016/j.quascirev.2016.04.002.

de Dios Teruel, J., Alcolea, A., Hernández, A., Ruiz, A.J.O., 2015. Comparison of chemical composition of enamel and dentine in human, bovine, porcine and ovine teeth. Arch. Oral Biol. 60 (5), 768–775.

Gagnon, M., Chew, A.E., 2000. Dietary Preferences in Extant African Bovidae. J. Mammal. 81 (2), 490–511. https://doi.org/10.1644/1545-1542(2000)081<0490:DPIEAB>2.0.CO;2.

Gatti, L., Lugli, F., Sciutto, G., Zangheri, M., Prati, S., Mirasoli, M., et al., 2022. Combining elemental and immunochemical analyses to characterize diagenetic alteration patterns in ancient skeletal remains. Sci. Rep. 12 (1), 5112. https://doi.org/10.1038/s41598-022-08979-3.

Giovas, C.M., Kamenov, G.D., Fitzpatrick, S.M., Krigbaum, J., 2016. Sr and Pb isotopic investigation of mammal introductions: Pre-Columbian zoogeographic records from the Lesser Antilles, West Indies. J. Archaeol. Sci. 69, 39–53.

Grimstead, D.N., Clark, A.E., Rezac, A., 2018. Uranium and vanadium concentrations as a trace element method for identifying diagenetically altered bone in the inorganic phase. J. Archaeol. Method Theory 25 (3), 689–704.

Harkins, W.D., 1917. The evolution of the elements and the stability of complex atoms. I. A new periodic system which shows a relation between the abundance of the elements and the structure of the nuclei of atoms. J. Am. Chem. Soc. 39 (5), 856–879.

Hillson, S., 2005. Teeth. Cambridge University Press.

Hinz, E.A., Kohn, M.J., 2010. The effect of tissue structure and soil chemistry on trace element uptake in fossils. Geochim. Cosmochim. Acta 74 (11), 3213–3231.

Hodgkins, J., le Roux, P., Marean, C.W., Penkman, K., Crisp, M., Fisher, E., Lee-Thorp, J., 2018. The role of ostrich in shaping the landscape use patterns of humans and hyenas on the southern coast of South Africa during the late Pleistocene. Multispecies Archaeology. Routledge.

Horsky, M., Irrgeher, J., Prohaska, T., 2016. Evaluation strategies and uncertainty calculation of isotope amount ratios measured by MC ICP-MS on the example of Sr. Anal. Bioanal. Chem. 408 (2), 351–367. https://doi.org/10.1007/s00216-015-9003-9.

Irrgeher, J., Prohaska, T., Sturgeon, E., Mester, Z., Yang, L., 2013. Determination of strontium isotope amount ratios in biological tissues using MC-ICPMS. Anal. Methods 5 (7), 1687–1694. https://doi.org/10.1039/C3AY00028A.

Irrgeher, J., Galler, P., Prohaska, T., 2016. 87Sr/86Sr isotope ratio measurements by laser ablation multicollector inductively coupled plasma mass spectrometry: Reconsidering matrix interferences in bioapatites and biogenic carbonates. Spectrochim. Acta B At. Spectrosc. 125, 31–42.

Jaouen, K., Beasley, M., Schoeninger, M., Hublin, J.-J., Richards, M.P., 2016. Zinc isotope ratios of bones and teeth as new dietary indicators: results from a modern food web (Koobi Fora, Kenya). Sci. Rep. 6 (1), 26281 https://doi.org/10.1038/srep26281.

Jochum, K.P., Garbe-Schönberg, D., Veter, M., Stoll, B., Weis, U., Weber, M., et al., 2019. Nano-powdered calcium carbonate reference materials: significant progress for microanalysis? Geostand. Geoanal. Res. 43 (4), 595–609. https://doi.org/10.1111/ggr.12292.

Kamenov, G.D., Lofaro, E.M., Goad, G., Krigbaum, J., 2018. Trace elements in modern and archaeological human teeth: Implications for human metal exposure and enamel diagenetic changes. J. Archaeol. Sci. 99, 27–34.

Keenan, S.W., Engel, A.S., 2017. Early diagenesis and recrystallization of bone. Geochim. Cosmochim. Acta 196, 209–223.

Kocsis, L., Trueman, C.N., Palmer, M.R., 2010. Protracted diagenetic alteration of REE contents in fossil bioapatites: Direct evidence from Lu–Hf isotope systematics. Geochim. Cosmochim. Acta 74 (21), 6077–6092. https://doi.org/10.1016/j.gca.2010.08.007.

Kohn, M.J., Schoeninger, M.J., Barker, W.W., 1999. Altered states: effects of diagenesis on fossil tooth chemistry. Geochim. Cosmochim. Acta 63 (18), 2737–2747.

Kowalik, N., Anczkiewicz, R., Wilczyński, J., Wojtal, P., Müller, W., Bondioli, L., Gasparik, M., 2020. Tracing human mobility in central Europe during the Upper Paleolithic using sub-seasonally resolved Sr isotope records in ornaments. Sci. Rep. 10 (1), 10386.

Kowalik, N., Anczkiewicz, R., Müller, W., Spötl, C., Bondioli, L., Nava, A., Matyszczak, M., 2023. Revealing seasonal woolly mammoth migration with spatially-resolved trace element, Sr and O isotopic records of molar enamel. Quat. Sci. Rev. 306, 108036.

Kubat, J., Nava, A., Bondioli, L., Dean, M.C., Zanolli, C., Bourgon, N., Müller, W., 2023. Dietary strategies of Pleistocene Pongo sp. and Homo erectus on Java (Indonesia). Nat. Ecol. Evol. 7 (2), 279–289.

Lee-Thorp, J.A., van der Merwe, N.J., 1991. Aspects of the chemistry of modern and fossil biological apatites. J. Archaeol. Sci. 18 (3), 343–354.

Leichliter, J.N., Lüdecke, T., Foreman, A.D., Duprey, N.N., Winkler, D.E., Kast, E.R., et al., 2021. Nitrogen isotopes in tooth enamel record diet and trophic level enrichment: Results from a controlled feeding experiment. Chem. Geol. 563, 120047 https://doi.org/10.1016/j.chemgeo.2020.120047.

Lodders, K., 2003. Solar system abundances and condensation temperatures of the elements. Astrophys J 591 (2), 1220.

Loewy, S.L., Valdes, J., Wang, H., Ingram, B., Miller, N.R., Medina, K.C., et al., 2020. Improved accuracy of U-series and radiocarbon dating of ostrich eggshell using a sample preparation method based on microstructure and geochemistry: a study from the Middle Stone Age of Northwestern Ethiopia. Quat. Sci. Rev. 247, 106525 https://doi.org/10.1016/j.quascirev.2020.106525.

MacFadden, B.J., DeSantis, L.R., Hochstein, J.L., Kamenov, G.D., 2010. Physical properties, geochemistry, and diagenesis of xenarthran teeth: prospects for interpreting the paleoecology of extinct species. Palaeogeogr. Palaeoclimatol. Palaeoecol. 291 (3–4), 180–189.

Martin, J.E., Tacail, T., Balter, V., 2017. Non-traditional isotope perspectives in vertebrate palaeobiology. Palaeontology 60 (4), 485–502. https://doi.org/10.1111/pala.12300.

Nelson, B.K., DeNiro, M.J., Schoeninger, M.J., De Paolo, D.J., Hare, P.E., 1986. Effects of diagenesis on strontium, carbon, nitrogen and oxygen concentration and isotopic composition of bone. Geochim. Cosmochim. Acta 50 (9), 1941–1949.

Pollard, A.M., Batt, C.M., Stern, B., Young, S.M., Young, S.M.M., 2007. Analytical Chemistry in Archaeology. Cambridge University Press.

Rey, L., Tacail, T., Santos, F., Rottier, S., Goude, G., Balter, V., 2022. Disentangling diagenetic and biogenic trace elements and Sr radiogenic isotopes in fossil dental enamel using laser ablation analysis. Chem. Geol. 587, 120608.

Reynard, B., Balter, V., 2014. Trace elements and their isotopes in bones and teeth: Diet, environments, diagenesis, and dating of archeological and paleontological samples. Palaeogeogr. Palaeoclimatol. Palaeoecol. 416, 4–16.

Samuelsen, J.R., Potra, A., 2020. Biologically available Pb: A method for ancient human sourcing using Pb isotopes from prehistoric animal tooth enamel. J. Archaeol. Sci. 115, 105079 https://doi.org/10.1016/j.jas.2020.105079.

Sato, I., Shimada, K., Ezure, H., Sato, T., 1995. Elemental analysis of deciduous and permanent incisor teeth in Bovidae. Jpn. J. Oral Biol. 37 (1), 9–18.

Sharp, W.D., Tryon, C.A., Niespolo, E.M., Fylstra, N.D., Tripathy-Lang, A., Faith, J.T., 2019. 230Th/U burial dating of ostrich eggshell. Quat. Sci. Rev. 219, 263–276. https://doi.org/10.1016/j.quascirev.2019.06.037.

Sponheimer, M., Lee-Thorp, J.A., DeRuiter, D.J., Smith, J.M., van der Merwe, N.J., Reed, K., et al., 2003. Diets of Southern African Bovidae: Stable Isotope Evidence. J. Mammal. 84 (2), 471–479. https://doi.org/10.1644/1545-1542(2003)084<0471:DOSABS>2.0.CO;2.

Stewart, B.A., Zhao, Y., Mitchell, P.J., Dewar, G., Gleason, J.D., Blum, J.D., 2020. Ostrich eggshell bead strontium isotopes reveal persistent macroscale social networking across late Quaternary southern Africa. Proc. Natl. Acad. Sci. 117 (12), 6453–6462. https://doi.org/10.1073/pnas.1921037117.

Trueman, C.N., Behrensmeyer, A.K., Tuross, N., Weiner, S., 2004. Mineralogical and compositional changes in bones exposed on soil surfaces in Amboseli National Park, Kenya: diagenetic mechanisms and the role of sediment pore fluids. J. Archaeol. Sci. 31 (6), 721–739.

Wathen, C.A., Isaksson, S., Lidén, K., 2022. On the road again—a review of pretreatment methods for the decontamination of skeletal materials for strontium isotopic and concentration analysis. Archaeol. Anthropol. Sci. 14 (3), 45. https://doi.org/10.1007/s12520-022-01517-2.

Weber, M., Lugli, F., Jochum, K.P., Cipriani, A., Scholz, D., 2018. Calcium carbonate and phosphate reference materials for monitoring bulk and microanalytical determination of Sr isotopes. Geostand. Geoanal. Res. 42 (1), 77–89. https://doi.org/10.1111/ggr.12191.

Weber, M., Lugli, F., Hattendorf, B., Scholz, D., Mertz-Kraus, R., Guinoiseau, D., Jochum, K.P., 2020. NanoSr – a new carbonate microanalytical reference material for in situ strontium isotope analysis. Geostand. Geoanal. Res. 44 (1), 69–83. https://doi.org/10.1111/ggr.12296.

Weber, K., Weber, M., Menneken, M., Kral, A.G., Mertz-Kraus, R., Geisler, T., et al., 2021. Diagenetic stability of non-traditional stable isotope systems (Ca, Sr, Mg, Zn) in teeth – an in-vitro alteration experiment of biogenic apatite in isotopically enriched tracer solution. Chem. Geol. 572, 120196 https://doi.org/10.1016/j.chemgeo.2021.120196.